Energy & Environmental Science

RSC Publishing

PAPER

View Article Online
View Journal

A membrane-free lithium/polysulfide semi-liquid battery for large-scale energy storage†

Cite this: DOI: 10.1039/c3ee00072a

Yuan Yang,‡[a] Guangyuan Zheng‡[b] and Yi Cui*[ac]

Large-scale energy storage represents a key challenge for renewable energy and new systems with low cost, high energy density and long cycle life are desired. In this article, we develop a new lithium/polysulfide (Li/PS) semi-liquid battery for large-scale energy storage, with lithium polysulfide (Li_2S_8) in ether solvent as a catholyte and metallic lithium as an anode. Unlike previous work on Li/S batteries with discharge products such as solid state Li_2S_2 and Li_2S, the catholyte is designed to cycle only in the range between sulfur and Li_2S_4. Consequently all detrimental effects due to the formation and volume expansion of solid Li_2S_2/Li_2S are avoided. This novel strategy results in excellent cycle life and compatibility with flow battery design. The proof-of-concept Li/PS battery could reach a high energy density of 170 W h kg^{-1} and 190 W h L^{-1} for large scale storage at the solubility limit, while keeping the advantages of hybrid flow batteries. We demonstrated that, with a 5 M Li_2S_8 catholyte, energy densities of 97 W h kg^{-1} and 108 W h L^{-1} can be achieved. As the lithium surface is well passivated by $LiNO_3$ additive in ether solvent, internal shuttle effect is largely eliminated and thus excellent performance over 2000 cycles is achieved with a constant capacity of 200 mA h g^{-1}. This new system can operate without the expensive ion-selective membrane, and it is attractive for large-scale energy storage.

Received 9th January 2013
Accepted 7th March 2013

DOI: 10.1039/c3ee00072a

www.rsc.org/ees

Broader context

Energy storage systems are crucial for extensive deployment of renewable energy, due to the intermittent nature of many forms of green energy, such as solar and wind systems. Low cost, high energy density and long cycle life are desired for large-scale energy storage. Rechargeable batteries are attractive among various strategies, as they are modular, environmentally friendly and not limited by location. Herein, we propose a new room-temperature lithium/polysulfide (Li/PS) semi-liquid battery, which has high energy density while maintaining the merits of hybrid flow batteries. In this system, lithium polysulfide (Li_2S_8) in ether-based solvent and passivated metallic lithium are used as the catholyte and the anode, respectively. This proof-of-concept Li/PS battery has a theoretical energy density of 170 W h kg^{-1} and 190 W h L^{-1} based on the mass and volume of catholyte and lithium. Excellent performance over 2000 cycles has been accomplished with constant capacity cycling at a capacity of 200 mA h g^{-1}, corresponding to 37 and 72 W h L^{-1} for full cells with 2.5 and 5 M catholyte, respectively, which is higher than that of conventional vanadium flow batteries. The system also has a low cost and low self-discharge rate.

Introduction

Energy storage systems are crucial for extensive deployment of renewable energy, due to the intermittent nature of many forms of green energy, such as solar and wind systems.[1–5] Low cost, high energy density and long cycle life are desired for large-scale energy storage. Rechargeable batteries are attractive among various strategies, as they are modular, environmentally friendly and not limited by location.[4] Among different chemistries explored, redox flow batteries and lead-acid batteries have relatively low cost but also low specific energy (20–50 W h kg^{-1}). Na/S batteries need to be operated at high temperature (300–350 °C).[6] New battery systems with exceptional performance are needed. Recently, our group has reported Prussian blue-like open framework materials with ultra-long cycle life although their specific energy is low (~30 W h kg^{-1}).[7–9] Several other groups also demonstrated a semi-solid flow battery based on the suspension of Li-ion battery materials.[10,11] The semi-solid system has a high energy density but may need more complexity in material preparation and system design than a conventional flow battery. A liquid metal battery was also reported with very high current density but it needs to be operated at 700 °C and shows a low voltage (~0.5 V).[12] Aqueous rechargeable Li-ion batteries also draw much attention due to their safety.[13–15] Herein, we propose a new room-temperature lithium/

[a]Department of Materials Science and Engineering, Stanford University, Stanford, California 94305, USA. E-mail: yicui@stanford.edu

[b]Department of Chemical Engineering, Stanford University, Stanford, California 94305, USA

[c]SLAC National Accelerator Laboratory, Stanford Institute for Materials and Energy Sciences, 2575 Sand Hill Road, Menlo Park, California 94025, USA

† Electronic supplementary information (ESI) available. See DOI: 10.1039/c3ee00072a

‡ These authors contributed equally to this work.

polysulfide (Li/PS) semi-liquid battery, which has high energy density while maintaining the merits of hybrid flow batteries. In this system, lithium polysulfide (Li_2S_8) in 1,3-dioxolane (DOL)/1,2-dimethoxyethane (DME) and passivated metallic lithium are used as the catholyte and the anode, respectively. The catholyte is only cycled between sulfur and Li_2S_4, but not to the insoluble Li_2S_2 and Li_2S phases. This proof-of-concept Li/PS battery has a theoretical energy density of 170 W h kg^{-1} and 190 W h L^{-1} based on the mass and volume of the catholyte and lithium. The $LiNO_3$ additive in the ether solvent helps form a uniform solid electrolyte interphase (SEI) that prevents parasitic reactions between polysulfide and lithium. Furthermore, as the catholyte is not discharged to insoluble Li_2S_2 and Li_2S, which is different from previous work on Li–S batteries, all adverse effects on cycling due to the formation and volume change of Li_2S_2 and Li_2S are avoided. Subsequently high coulomb efficiency and long cycle life are achieved. This high quality SEI also acts as a solid electrolyte layer, so that the polysulfide catholyte could directly contact the lithium anode but not react with it. This unique property allows the system to work without the expensive ion-selective membrane and significantly lowers the cost. Excellent performance over 2000 cycles has been accomplished with constant capacity cycling at a capacity of 200 mA h g^{-1}, corresponding to 37 and 72 W h L^{-1} for full cells with 2.5 and 5 M catholyte, respectively, which is higher than that of vanadium flow batteries.[2] Constant voltage cycling also shows capacity retention as high as 75% for 500 cycles with a specific capacity of 335 mA h g^{-1}. Recently Zhang and Read,[16] and Demir-Cakan *et al.*[17] reported an Li–S battery with a polysulfide catholyte. Though improved performance was observed, the nucleation and volume change of insoluble Li_2S_2/Li_2S still significantly deteriorate the cycle life, as the catholyte is discharged to the lower plateau. Apparent capacity fading is observed within 50–100 cycles. Our strategy of using narrow voltage window successfully avoids all issues related to Li_2S_2/Li_2S and the system is compatible with the flow battery design. We noted that, while preparing the manuscript, a similar idea has been proposed by the Arumugam Manthiram group although there has not been experimental demonstration of this idea.[18]

Experimental

Li_2S powder and 0.75 mm thick lithium strip (99.9%) were purchased from Alfa Aesar and all other materials were received from Sigma Aldrich. To prepare lithium polysulfide solution, stoichiometric amounts of Li_2S and sulfur were mixed together with a nominal formula of Li_2S_8 and stirred in dioxolane/dimethoxyethane solvent (DOL/DME m/m = 1 : 1) at 60 °C overnight. 5 M and 2.5 M solutions were used in this study. All molarities in this report are based on the amount of sulfur in the solution. The passivation layer on the surface of the lithium anode was realized by soaking the lithium strip in 0.5 M lithium bis(trifluoromethanesulfonyl)imide (LiTFSI) in DOL/DME solution with 1 wt% $LiNO_3$ additive for 1.5 hours. A 2032 coin cell was used to evaluate the performance of this proof-of-concept semi-liquid cell. Carbon fiber paper discs with a diameter of 1.25 cm (AvCarb™ P75) served as the current collector for the catholyte, and a piece of common porous Li-ion battery separator (Asahi) was used to separate lithium and carbon electrodes. It should be noticed that the purpose of using a separator is only to avoid shorting between the carbon electrode and lithium, but not selectively transport lithium ions. Samples were tested with a multi-channel Arbin battery tester. The voltage range for cycling is 2.15–2.8 V. In all measurements, 1 C rate is defined as the reaction of 0.5 Li^+ per sulfur in one hour (S → Li_2S_4 per hour), which is 418 mA g^{-1}.

Results and discussion

The schematic of the proposed Li/PS battery is shown in Fig. 1a. Lithium foils are used as an anode while liquid lithium polysulfide solution is used as a catholyte with carbon-paper as the current collector. The design is similar to a hybrid flow battery, such as the Zn–bromine system.[4] In operation, polysulfide solution continually flows through the electrode stacks to generate or store electricity, while the catholyte drains back to the reservoir tank in downtime. Such a design has merits of modularity,

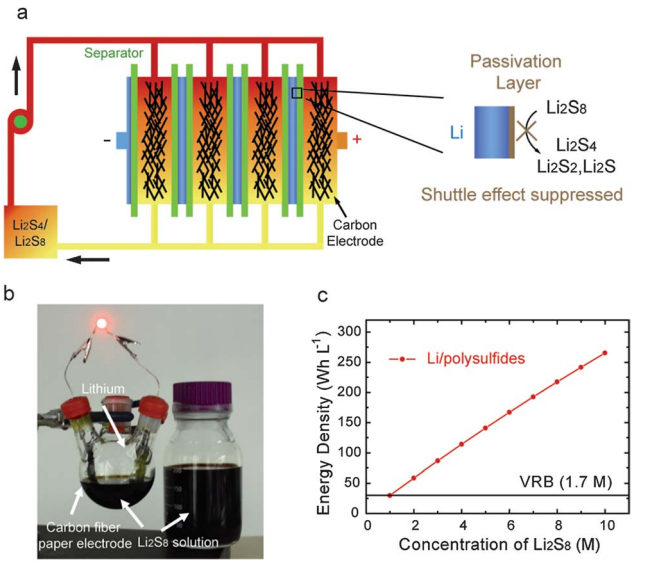

Fig. 1 Design principle of the Li/PS battery. (a) The schematic illustrating the structure of the Li/PS battery. Polysulfides flow through the system during operation and are stored in the tank in downtime. Magnified scheme on the right: the SEI passivation layer has a high resistance towards internal reaction between PS and lithium due to the presence of $LiNO_3$. Consequently the shuttle effect is significantly suppressed. The narrow voltage window avoids the formation of insoluble Li_2S_2/Li_2S and leads to excellent cycle life. (b) An experimental demonstration of the membrane-free Li/PS battery with lithium and the carbon fiber electrode soaked in Li_2S_8 solution. The Li_2S_8 solution can be prepared easily by mixing stoichiometric amounts of Li_2S and sulfur in ether-based solvent. Additional polysulfides can be added from an external reservoir. (c) The volumetric energy density of the Li/PS system *versus* concentration of sulfur in the catholyte. The capacity of lithium is set to 2000 mA h g^{-1} and 1000 mA h cm^{-3} to take the extra lithium needed for practical operation into consideration. The specific capacity between sulfur and Li_2S_4 is 418 mA h g^{-1}. The black line shows the energy density of the vanadium flow battery based on the vanadium catholyte and analyte only (30 W h L^{-1}). The concentrations of both catholyte and analyte are supposed to be 1.7 M, which is the commonly used stability limit for vanadium flow batteries.[28]

transportability, flexibility in design and scalability.[3] The liquid nature of polysulfides also avoids issues of volume expansion and poor kinetics of Li_2S in conventional Li/S batteries.[19–23] To prevent direct reaction between the highly reactive lithium and polysulfides, we utilize the recently developed $LiNO_3$ electrolyte additive to form a passivating layer on the lithium surface. The effect of the $LiNO_3$ additive is first reported by Aurbach *et al.*[24] in Li/S batteries and confirmed by other works.[25–27] The coulomb efficiency of Li/S batteries with the $LiNO_3$ additive is improved significantly from less than 90% to more than 99%. $LiNO_3$ is probably reduced to insoluble Li_xNO_y species at the lithium surface and oxidizes the polysulfides in solution to Li_xSO_y species, preventing the continuous electron transfer from lithium to polysulfides in solutions.[24] This passivation layer dramatically improves the coulomb efficiency and significantly reduces self-discharge in the Li/PS system (Fig. 1a). To form a uniform passivation layer, the lithium anode is first soaked in 0.5 M LiTFSI in DOL/DME electrolyte with 1% $LiNO_3$ additive for 1.5 hours, followed by drying and assembled into a full cell. A simple demonstration of the membrane-free Li/PS battery is shown in Fig. 1b by soaking the carbon fiber paper electrode and lithium in a polysulfide solution (2.5 M Li_2S_8 in DOL/DME m/m = 1 : 1). The Li_2S_8 solution can be easily prepared by stirring stoichiometric amounts of Li_2S and sulfur in DOL/DME solvent. 200 mL of the solution was prepared and stored in a glass bottle, which serves as a reservoir for additional polysulfides.

The Li/PS battery is attractive as it has higher energy density compared to other redox flow batteries (RFBs). The electrochemical reactions involved in the Li/PS system include:[29,30]

$$S_{8\ (solid)} + 2e^- \rightarrow S_8^{2-}{}_{(liquid)}$$

$$3S_8^{2-}{}_{(liquid)} + 2e^- \rightarrow 4S_6^{2-}{}_{(liquid)}$$

$$2S_6^{2-}{}_{(liquid)} + 2e^- \rightarrow 3S_4^{2-}{}_{(liquid)}$$

Except sulfur, all other phases are readily soluble in the solvent. The specific capacity within the range between Li_2S_4 and sulfur is 418 mA h g^{-1} based on the mass of sulfur in the catholyte. Lithium has a high theoretical specific capacity of 3860 mA h g^{-1}. In addition, the average discharge voltage of the reactions is 2.30 V, which is higher than the stability voltage dictated by many aqueous electrolytes used in other redox flow batteries. Lithium polysulfide has high solubility in ether-based electrolyte, with ~7 M in DOL/DME solution and ~10 M in tetrahydrofuran.[31] In comparison, the concentration of vanadium species in conventional vanadium redox batteries (VRBs) is typically not higher than 1.7 M to avoid stability issues.[2,28] Fig. 1c and S1† show the volumetric and gravimetric energy densities of Li/PS batteries, respectively. In calculation, the capacity of lithium is set to 2000 mA h g^{-1} or 1000 mA h cm^{-3} (half of its theoretical capacity) to take into account the low coulomb efficiency of lithium. When a 5 M polysulfide solution is used, the energy density reaches 149 W h L^{-1} (133 W h kg^{-1}), which is about five times that of the vanadium redox battery (VRB) (see ESI for detailed calculation†).

The electrochemical performance of the Li/PS system is shown in Fig. 2. All electrochemical tests in this paper were done in the 2032 coin cell configuration (see Experimental). Fig. 2a shows the voltage profile of a Li/PS cell with 35 μL 5 M Li_2S_8 solution as the catholyte at a current of 0.8 C (334 mA g^{-1} or 1.5 mA cm^{-2}). The initial discharge capacity is 172 mA h g^{-1}, which is consistent with the capacity to reduce Li_2S_8 to Li_2S_4. The subsequent charge–discharge profiles are the same as common sulfur, which suggests that sulfur forms at the end of charge. The second discharge reaches a capacity of 295 mA h g^{-1} sulfur, corresponding to a capacity of 48 mA h cm^{-3} for the whole catholyte. By taking into account both the catholyte and lithium, the energy density of the system reaches 95 W h kg^{-1} and 106 W h L^{-1}. These values are three times that of the vanadium flow battery with a concentration of 1.7 M.[2] The average discharge and charge voltage are 2.45 and 2.30 V, respectively, indicating that the reaction is highly reversible.

Results on constant voltage cycling of the Li/PS system are shown in Fig. 2b. Two different concentrations, 2.5 M and 5 M, are investigated at 0.8 C rate. 2.5 wt% $LiNO_3$ additive is added to the solution. The 5 M sample reaches a capacity of 300 mA h g^{-1} (based on sulfur) at the beginning while the 2.5 M polysulfide solution has a higher initial capacity of 335 mA h g^{-1}, since lower concentration of the active material leads to a lower current at the same C rate, and thus a smaller overpotential and higher specific capacity. The corresponding energy densities of the cell are 108 W h L^{-1} (97 W h kg^{-1}) and 61 W h L^{-1} (59 W h kg^{-1}) for 5 M and 2.5 M catholytes, respectively. The discharge capacities after 500 cycles are 175 and 252 mA h g^{-1}, respectively. The corresponding capacity fading rate is as low as 8.4% and 5.0% per 100 cycles. The cycling data show potential for applications in grid-level energy storage, and optimization on additives and solvents could further enhance the cycle life. The

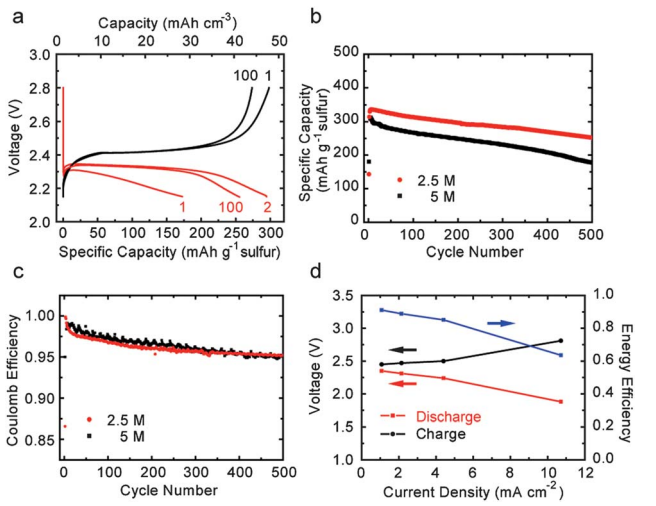

Fig. 2 Electrochemical characteristics of the Li/PS system. (a) The voltage profile of a cell with 35 μL 5 M Li_2S_8 catholyte at 0.8 C (334 mA g^{-1} or 1.5 mA cm^{-2}). The cycling performance (b) and coulomb efficiency (c) of the system. 2.5 wt% $LiNO_3$ is added to both solutions, and the volume of catholyte in each sample is 35 μL. (d) The charge/discharge voltage of the Li/PS full cell at different current densities and the corresponding energy efficiency.

cells also exhibited high coulomb efficiency at around 99% initially, and stabilized at around 95% even after 500 cycles. This indicates that the lithium surface is well passivated and thus the shuttle effect is largely eliminated. In contrast, cells without the $LiNO_3$ additive cannot be properly charged due to the strong shuttle effect (Fig. S2†). The corresponding coulomb efficiency is only 15%.

The power capability and energy efficiency of the Li/PS system are also studied. Fig. 2d shows the discharge and charge voltage of the full cell at different current densities. The voltage is selected as the midpoint potential for a 200 mA h g^{-1} constant capacity cycling at different rates. At 1 mA cm^{-2} (2.3 mW cm^{-2}), the voltage hysteresis is as low as 100 mV, leading to a high voltage efficiency of 96% and energy efficiency of 91%. When the current is increased to 4.4 mA cm^{-2} (10 mW cm^{-2}), the discharge/charge voltage remains at 2.24 V and 2.5 V, respectively. The corresponding voltage efficiency is still 90% and the energy efficiency reaches 85%. In comparison, the energy efficiency of common flow batteries is only 65–80%.[2] Moreover, as both sides of the lithium and carbon current collector could be used to generate power in a real system, the real current density per footprint area of the electrode could be doubled at the same energy efficiency.

Constant capacity cycling was also carried out. In this test, we try to limit the cycling within the range of liquid phases ($Li_2S_8 \leftrightarrow Li_2S_4$) so that solid–liquid phase transformation does not occur, which is known to deteriorate the cycle life. The cell is first discharged to 2.15 V and then the charging capacity is kept at 200 mA h g^{-1}. The voltage cut-off for all following discharges is 2.15 V. At 200 mA h g^{-1} capacity, the energy densities are 37 and 72 W h L^{-1} for the cells with 2.5 M and 5 M catholyte, respectively (Fig. 3). Although a slight capacity drop is observed at the beginning of cycling, as the coulomb efficiency decreases in initial cycles, both 5 M and 2.5 M samples show steady cycling afterwards. For the 2.5 M sample, the capacity remains at 193 mA h g^{-1} after 2000 cycles, with a coulomb efficiency of 96.5%. The prototype cell can be charged–discharged for more than 2400 cycles before a significant increase in maximum charged voltage (MCV) is observed. The discharge capacity of the 5 M sample remains at 189 mA h g^{-1} after 1500 cycles. These cycling data are comparable with current state-of-the-art flow batteries. The maximum charged voltage (MCV) is almost constant over about 90% of the whole cycle life, allowing feasible control over voltage delivery. The excellent cycling performance of the polysulfide electrode originates from the fact that all detrimental effects related to solid state Li_2S/Li_2S are eliminated by controlling the discharge voltage cut-off. Our results also indicate that when the $LiNO_3$ additive is present, polysulfide dissolution and shuttle effect are not the most important issues. Instead, phase nucleation and volume change of insoluble Li_2S_2 and Li_2S are likely to play a significant role in capacity fading of traditional Li–S batteries.

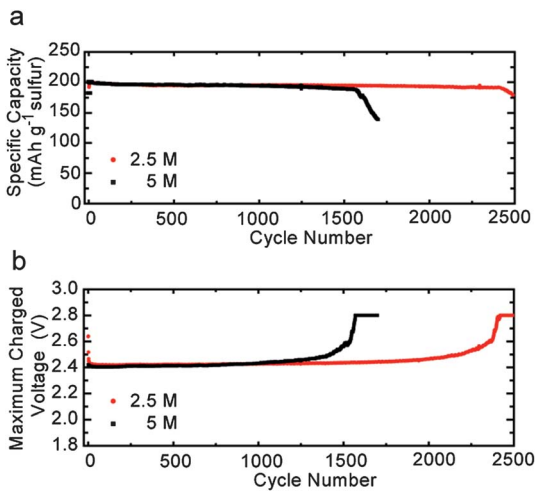

Fig. 3 Constant capacity cycling of Li/PS cells. (a) The discharge capacity *versus* cycle number for constant capacity cycling where the charge capacity is set to 200 mA h g^{-1} and the discharge cut-off is set to 2.15 V. (b) The maximum charge voltage *versus* cycle number in the constant capacity cycling. 25 μL catholyte with 2.5 wt% $LiNO_3$ was used in the tests.

In order to understand the mechanisms behind the capacity decay and guide further optimization of the system, effects of various parameters on the cycle life and coulomb efficiency are studied. In our investigation, the cycle life is evaluated as the capacity decay from the 100th to the 200th cycle in constant voltage cycling (2.15–2.8 V), and the coulomb efficiency used for comparison is based on the value after stabilization. We found that a lower concentration of polysulfides leads to a better cycle life (Fig. 4a). The capacity decay rate for the 2.5 M catholyte is mostly within 5–7.5% per 100 cycles, while the majority of samples with 5 M catholyte show a decay rate of around 10–15% per 100 cycles. There are two possible reasons: (1) direct reaction between polysulfides and lithium is slower at lower concentration, (2) at the same current rate, low concentration means low current, which causes less damage to the lithium anode. Other factors, such as current rate, concentration of $LiNO_3$ and volume of catholyte, do not show statistically significant influence on the cycle life.

The major contributing factor influencing coulomb efficiency is found to be the $LiNO_3$ concentration. Both samples with 1 wt% and 2.5 wt% of $LiNO_3$ additive showed nearly 100% coulomb efficiency at the beginning, but the value decreases to 85–90% for samples with 1% additive while those with 2.5% $LiNO_3$ stabilized at around 95–97% (Fig. 4b). This observation could be explained as follows. At the beginning, the passivation layer on lithium results in a high coulomb efficiency. After cycling, lithium gradually exposes to the catholyte due to the re-deposition of lithium in charging and cracks of the lithium film arising from the volume change. Then $LiNO_3$ and polysulfides compete with each other to react with the exposed fresh lithium surface. A higher concentration of $LiNO_3$ passivates the lithium surface faster so there is less reaction between lithium and polysulfides. Consequently higher coulomb efficiency is achieved. A higher current rate also favors higher coulomb efficiency (Fig. 4d), which is well established by previous reports.[30,32] The concentration of polysulfides and volume have no statistically significant effect on coulomb efficiency, which can be explained by the mathematical model developed by Mikhaylik and Akridge.[30] In their model, the level of the shuttle effect is related to the parameter $f_c = kq_H[S_{total}]/I$, where k is the

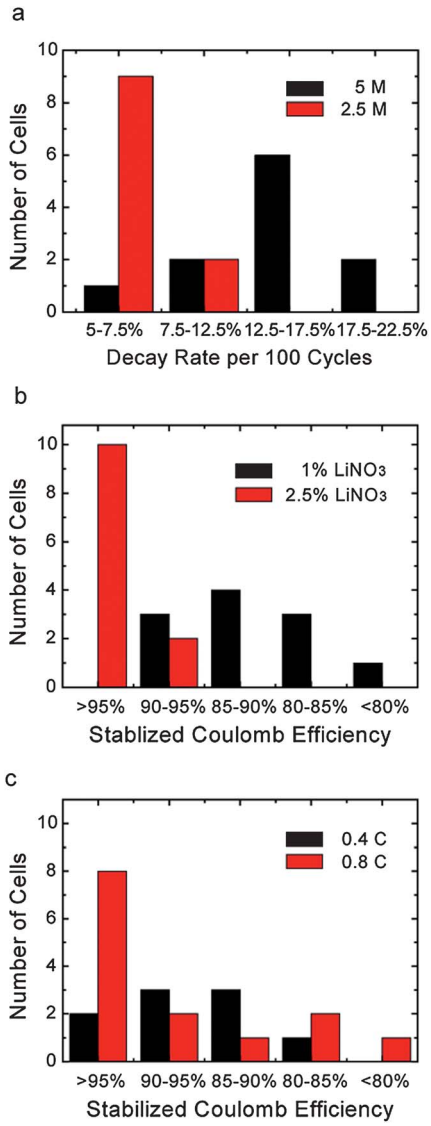

Fig. 4 The effect of different factors on cycle life and coulomb efficiency. (a) The statistics on the effect of polysulfide concentration on the decay rate per 100 cycles. The decay rate is defined as $1 - C_{200\text{th discharge}}/C_{100\text{th discharge}}$, where C means the specific capacity. Statistics on the effects of (b) $LiNO_3$ concentration and (c) current rate on stabilized coulomb efficiency. Details of the samples used in the statistics can be found in the ESI.†

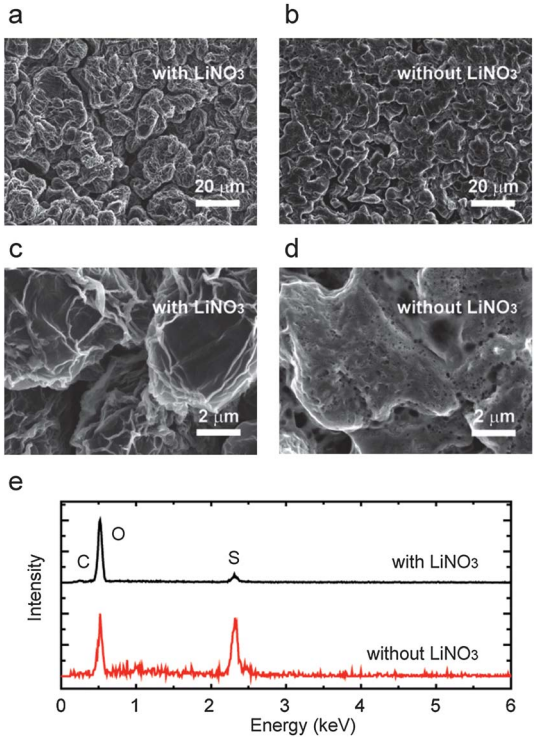

Fig. 5 SEM characterizations of the lithium surface after cycling. The SEM images of the lithium anode with (a) and without (b) $LiNO_3$ additive. (c and d) The zoom-in images of (a) and (b), respectively. (e) The corresponding energy dispersive spectrum of the lithium surface with (black) and without (red) $LiNO_3$ additive. The spectrum is normalized to the intensity of oxygen.

heterogeneous reaction constant, q_H is the high plateau sulfur specific capacity, $[S_{total}]$ is the total sulfur concentration in the catholyte and I is the absolute value of the current. At the same C rate, $[S_{total}]/I$ is a constant no matter how $[S_{total}]$ and volume change, and thus the concentration of polysulfides and volume should not affect coulomb efficiency.

The effect of the $LiNO_3$ additive is further examined by characterizing the lithium surface by scanning electron microscopy (SEM), as illustrated in Fig. 5. The surface of the lithium anode was characterized after 100 cycles with a 5 M Li_2S_8 catholyte. Though both samples show a particulate surface (Fig. 5a and b), the lithium surface without additive is more porous (Fig. 5d) while the one with $LiNO_3$ is much smoother at the microscale (Fig. 5c). The porous surface indicates that lithium is aggressively corroded by polysulfides in the catholyte without passivation, resulting in inhomogeneous local current densities. The energy-dispersive X-ray spectroscopy results showed a strong sulfur peak for the sample without the $LiNO_3$ additive, indicating the formation of insoluble Li_2S or Li_2S_2 on the surface of lithium. In contrast, a very weak sulfur signal is detected for samples with 2.5 wt% $LiNO_3$ additives. These results also explain why there is a strong correlation between the concentration of $LiNO_3$ and the stabilized coulomb efficiency (Fig. 4b).

The system's stability against overdischarge is also investigated. We discharge extra 100 mA h g^{-1} capacity every 20 cycles and check whether the cycling performance degrades. The overdischarged capacity is 1/3 of that in normal discharge. In ordinary cycling, as the low cut-off is 2.15 V, Li_2S_8 is not totally converted to the Li_2S_4 phase. As a result, the overdischarged capacity includes two parts, as shown in Fig. 6a. The first part is to continually reduce all polysulfides to Li_2S_4, which counts for ~65 mA h g^{-1}. The second part lasts for ~35 mA h g^{-1}, which is the conversion of soluble Li_2S_4 to insoluble Li_2S_2 phase, as indicated by the flat line at the end of the discharge curve. The corresponding cycling performance is shown in Fig. 6b. No notable degradation is observed, especially after the system becomes stabilized after 50 cycles. For example, the capacity fading rate is only 9.0% per 100 cycles between the 80th and 120th cycles, which is similar to cells without overdischarging. Moreover, no obvious drop in capacity or faster fading is

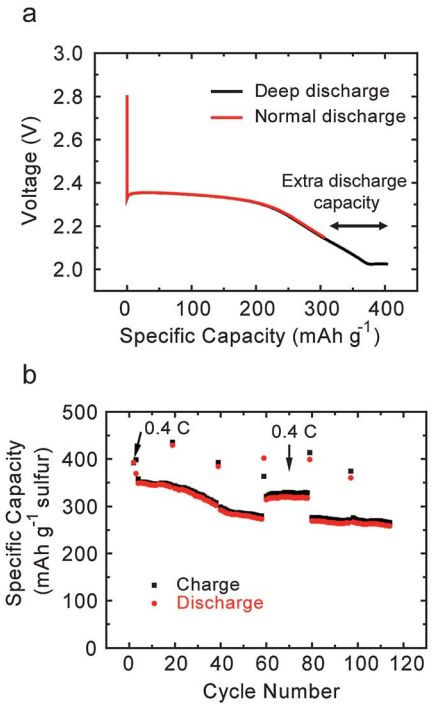

Fig. 6 Overdischarge test of the Li/PS cell. (a) The voltage profile of normal discharge and deep discharge. Extra 100 mA h g^{-1} is discharged, and phase transformation from soluble polysulfide to insoluble solid Li_2S_2 occurs in the deep discharge. (b) The corresponding cycling performance. Overdischarge is applied every 20 cycles. The current rate is 0.8 C except those marked with arrows. The cell used in this test has a 5 M Li_2S_8 catholyte solution and 2.5 wt% $LiNO_3$ additive. The volume of the catholyte is 25 μL.

observed after overdischarge. This suggests that the Li/PS battery has a good resistance to moderate level of overdischarge. We also calculate changes in Gibbs free energy of reactions between various polysulfides. It turns out that even if insoluble Li_2S and Li_2S_2 phases precipitate out of the catholyte in deep overdischarge, they can chemically react with Li_2S_8 and sulfur and dissolve in the ether solvent again (see ESI for details†). This is different from the solubility concern in vanadium flow batteries and should represent a minor issue for cell operation and system design.

One concern for the Li/PS battery is the possibility of forming solid phases at the end of charge and discharge. Solid sulfur forms at full charge based on the capacity obtained. However, as it is formed electrochemically, the sulfur phase sticks onto the carbon current collector, which is similar to the electroplating of zinc in a zinc–bromine hybrid flow battery. This indicates that sulfur does not form particles within the solution. Consequently it should have little adverse effect on the circulation of the catholyte.

At full discharge, Li_2S_8 is reduced to Li_2S_6 and Li_2S_4. We found that the solubility of chemically prepared Li_2S_4 is only ~2.5 M. Though electrochemically formed species could have different properties from their chemically prepared counterparts, this generates concerns on the solubility of the discharged species. To avoid the possible formation of precipitates, the voltage cut-off is limited to 2.15 V, which corresponds to a discharge capacity of ~300 mA h g^{-1} for the 5 M catholyte. Consequently, ~90% of sulfur remains in the form of Li_2S_6, which has a much higher solubility in the solvent so that precipitate should not form.

To further address this issue, we performed both experiments and theoretical calculations. Our conclusion is that the reduced products should not precipitate out. Even if a solid precipitate forms, it can be dissolved spontaneously in charge. First, two experimental tests were performed to check the existence of possible precipitates. In the first one, a discharged cell with 0.4 mL Li_2S_8 catholyte was opened and no precipitate was observed even after 36 hours. The second experiment is to rest the cell at the discharged state for 3 days and then check the discharge capacity in the following cycles. The change in capacity is not detectable (<1%), which suggests that precipitates are unlikely to form or they have minimum effect on the cell performance. Furthermore, theoretical calculations show that thermodynamically Li_2S_4 can react with sulfur to form Li_2S_8, which is readily soluble in the ether solvent (see ESI for detailed calculation†). As a result, Li_2S_4 precipitates could be consumed chemically in the charge cycle. In addition, 2.5 M polysulfide catholyte with a capacity of 330 mA h g^{-1} already leads to a high energy density of 60 W h L^{-1} and 58 W h kg^{-1}, about twice that of the VRB. This means that even if the concentration is limited to the entirely safe range regarding solubility, the energy density is already very attractive. It should be noted that the real flow battery system also includes pumps and plumbing, which decrease the energy density of the entire system.

The self-discharge behavior of the Li/PS system is also investigated. A seven-day resting shows an average self-discharge rate of 6.5% per day in the coin cell prototype (Fig. S3†). The equivalent permeation rate of active species at the Li/PS interface is only 10^{-6} cm min^{-1}, much lower than that in the vanadium-based system, which is in the order of 5×10^{-5} cm min^{-1} for the common Nafion membrane[33] (see ESI for details†). This indicates that the self-discharge rate in the Li/PS system is much less than that of the vanadium system. The result also demonstrates the high quality of the passivation layer on the lithium surface. Moreover, the capacity could be fully recovered in the following cycle, indicating that the self-discharge does not damage the rechargeability of the battery. Optimization of electrolyte additives, polysulfide concentration and solvent composition could further reduce the self-discharge rate.

Cost analysis shows that the Li/PS system is attractive. The expense on all raw materials is \$45 kW h^{-1}, which is less than that in VRBs (\$50–110 kW h^{-1} for vanadium materials)[34] and the total cost of the flow battery (\$180–250 kW h^{-1}).[4] The cost per power is also as low as \$145 kW^{-1} based on the cost of active materials, carbon current collectors and separators, which is reasonable for practical operations (see ESI for details†). Moreover, the unique property of SEI also makes the system free from the high-cost ion exchange membrane, which is the most expensive component in flow batteries (\$100–250 m^{-2}).[4,28,35] It should be noted that extra cost needs to be considered as safety protection is needed due to the use of organic electrolytes.

Conclusion

In this report, we develop a new lithium/polysulfide semi-liquid battery. This proof-of-concept Li/PS battery can reach 170 W h kg^{-1} and 190 W h L^{-1} at the solubility limit (7 M polysulfide catholyte). Experimentally we achieve an energy density of 108 W h L^{-1} and 97 W h kg^{-1} based on the mass of the polysulfide catholyte and lithium. The cost of raw materials in this system is as low as \$45 kW h^{-1} and \$145 kW^{-1}. Moreover, no expensive ion-selective membrane is needed for this system. Cycle life over 2000 cycles has been achieved in constant capacity cycling with a discharge capacity of 195 mA h g^{-1}, corresponding to 37 and 72 W h L^{-1} for full cells with 2.5 and 5 M catholyte, respectively. Constant voltage cycling also shows retention as high as 75% for 500 cycles with a capacity of 335 mA h g^{-1}. There are two key reasons for the good cycle life of this system: (1) narrow voltage window to avoid the formation and volume change of solid state Li_2S_2/Li_2S, which has not been reported in previous experiments and (2) the formation of the solid-electrolyte-like passivation layer on the lithium surface, which prevents the continuous electron transfer from Li to polysulfides in solution. Issues such as formation of possible insoluble phases in the catholyte and self-discharge are also discussed. This new system shows attractive and promising performance for large scale energy storage.

Acknowledgements

This work was supported as part of the Joint Center for Energy Storage Research, an Energy Innovation Hub funded by the U. S. Department of Energy, Office of Science, Basic Energy Sciences. G.Z. acknowledges financial support from Agency for Science, Technology and Research (A*STAR), Singapore. Portions of this research were carried out at the Stanford Synchrotron Radiation Lightsource, a national user facility operated by Stanford University on behalf of the U.S. Department of Energy, Office of Basic Energy Sciences.

References

1 M. Z. Jacobson, *Energy Environ. Sci.*, 2009, **2**, 148–173.
2 Z. Yang, J. Zhang, M. C. W. Kintner-Meyer, X. Lu, D. Choi, J. P. Lemmon and J. Liu, *Chem. Rev.*, 2011, **111**, 3577–3613.
3 C. Ponce De Leon, A. Frias-Ferrer, J. Gonzalez-Garcia, D. A. Szanto and F. C. Walsh, *J. Power Sources*, 2006, **160**, 716–732.
4 M. Skyllas-Kazacos, M. H. Chakrabarti, S. A. Hajimolana, F. S. Mjalli and M. Saleem, *J. Electrochem. Soc.*, 2011, **158**, R55.
5 B. Dunn, H. Kamath and J.-M. Tarascon, *Science*, 2011, **334**, 928–935.
6 X. Lu, G. Xia, J. P. Lemmon and Z. Yang, *J. Power Sources*, 2010, **195**, 2431–2442.
7 C. D. Wessells, R. A. Huggins and Y. Cui, *Nat. Commun.*, 2011, **2**, 550.
8 C. D. Wessells, S. V. Peddada, R. A. Huggins and Y. Cui, *Nano Lett.*, 2011, **11**, 5421–5425.
9 M. Pasta, C. D. Wessells, R. A. Huggins and Y. Cui, *Nat. Commun.*, 2012, **3**, 1149.
10 M. Duduta, B. Ho, V. C. Wood, P. Limthongkul, V. E. Brunini, W. C. Carter and Y.-M. Chiang, *Adv. Energy Mater.*, 2011, 511–516.
11 S. Hamelet, T. Tzedakis, J. B. Leriche, S. Sailler, D. Larcher, P. L. Taberna, P. Simon and J. M. Tarascon, *J. Electrochem. Soc.*, 2012, **159**, A1360–A1367.
12 D. J. Bradwell, H. Kim, A. H. C. Sirk and D. R. Sadoway, *J. Am. Chem. Soc.*, 2012, **134**, 1895–1897.
13 Q. Qu, L. Fu, X. Zhan, D. Samuelis, J. Maier, L. Li, S. Tian, Z. Li and Y. Wu, *Energy Environ. Sci.*, 2011, **4**, 3985–3990.
14 W. Tang, L. Liu, Y. Zhu, H. Sun, Y. Wu and K. Zhu, *Energy Environ. Sci.*, 2012, **5**, 6909–6913.
15 W. Tang, X. Gao, Y. Zhu, Y. Yue, Y. Shi, Y. Wu and K. Zhu, *J. Mater. Chem.*, 2012, **22**, 20143–20145.
16 S. S. Zhang and J. A. Read, *J. Power Sources*, 2012, **200**, 77–82.
17 R. Demir-Cakan, M. Morcrette, Gangulibabu, A. Gueguen, R. Dedryvere and J.-M. Tarascon, *Energy Environ. Sci.*, 2013, **6**, 176–182.
18 A. Manthiram, Y. Fu and Y.-S. Su, *Acc. Chem. Res.*, 2012, DOI: 10.1021/ar300179v.
19 X. L. Ji and L. F. Nazar, *J. Mater. Chem.*, 2010, **20**, 9821–9826.
20 P. G. Bruce, S. A. Freunberger, L. J. Hardwick and J.-M. Tarascon, *Nat. Mater.*, 2012, **11**, 19–30.
21 X. L. Ji, K. T. Lee and L. F. Nazar, *Nat. Mater.*, 2009, **8**, 500–506.
22 Y. Yang, G. Zheng and Y. Cui, *Chem. Soc. Rev.*, 2013, **42**, 3018–3032.
23 Z. W. Seh, W. Li, J. J. Cha, G. Zheng, Y. Yang, M. T. McDowell, P.-C. Hsu and Y. Cui, *Nat. Commun.*, 2013, **4**, 1331.
24 D. Aurbach, E. Pollak, R. Elazari, G. Salitra, C. S. Kelley and J. Affinito, *J. Electrochem. Soc.*, 2009, **156**, A694.
25 G. Zheng, Y. Yang, J. J. Cha, S. S. Hong and Y. Cui, *Nano Lett.*, 2011, **11**, 4462–4467.
26 X. Liang, Z. Wen, Y. Liu, M. Wu, J. Jin, H. Zhang and X. Wu, *J. Power Sources*, 2011, **196**, 9839–9843.
27 C. Barchasz, J.-C. Leprêtre, F. Alloin and S. Patoux, *J. Power Sources*, 2011, **199**, 322–330.
28 L. Li, S. Kim, W. Wang, M. Vijayakumar, Z. Nie, B. Chen, J. Zhang, G. Xia, J. Hu, G. Graff, J. Liu and Z. Yang, *Adv. Energy Mater.*, 2011, **1**, 394–400.
29 H. Yamin and E. Peled, *J. Power Sources*, 1983, **9**, 281–287.
30 Y. V. Mikhaylik and J. R. Akridge, *J. Electrochem. Soc.*, 2004, **151**, A1969–A1976.
31 R. D. Rauh, F. S. Shuker, J. M. Marston and S. B. Brummer, *J. Inorg. Nucl. Chem.*, 1977, **39**, 1761–1766.
32 J. Guo, Y. Xu and C. Wang, *Nano Lett.*, 2011, **11**, 4288–4294.
33 J. Xi, Z. Wu, X. Qiu and L. Chen, *J. Power Sources*, 2007, **166**, 531–536.
34 T. Nguyen and R. F. Savinell, *Electrochem. Soc. Interface*, 2010, **19**, 54–56.
35 B. Schwenzer, J. Zhang, S. Kim, L. Li, J. Liu and Z. Yang, *ChemSusChem*, 2011, **4**, 1388–1406.